Artificial Organs

WILEY

Artificial Organs

MAIN TEXT OPEN ACCESS

Ex Vivo Preservation of Porcine Vascularized Composite Soft Tissue Allografts

Abigail Meyers | Varun Lingaiah Kopparthy | Jacob Lammers | Mazen Al-Malak | Brian Figueroa | Ying Ku | Lianne Mulvihill | Ryan Khalaf | Jose Reyes | Diane Jo | R'ay Fodor | Payam Sadeghi | Antonio Rampazzo | Bahar Bassiri Gharb

Cleveland Clinic Department of Plastic Surgery, Cleveland, USA

Correspondence: Bahar Bassiri Gharb (bassirb@ccf.org)

Received: 8 September 2024 | **Revised:** 12 January 2025 | **Accepted:** 31 January 2025

Funding: This work was supported by Lerner Research Institute, Cleveland Clinic.

Keywords: ex vivo perfusion | ex vivo preservation | flap perfusion | vascularized composite allografts

ABSTRACT

Introduction: The aim of this study was to evaluate ex vivo perfusion (EVP) for vascularized composite tissue preservation. We hypothesized that EVP could maintain allografts in near-physiologic conditions for ≥24 h.

Methods: Twenty superior epigastric artery perforator-based abdominal flaps were procured from 10 Yorkshire pigs. Flaps were preserved for 12 h ($n=5$) or 24 h ($n=5$) using EVP with an oxygenated colloid solution containing HBOC-201 oxygen carrier (HbO_2 Therapeutics, Souderton, PA). Contralateral flaps were cold storage controls (4°C) ($n=10$). Hemodynamics, temperature, gases, metabolites, electrolytes, indocyanine green (ICG) angiography, and weight were analyzed. Biopsies were taken every 6 h for histology.

Results: Ischemia time was 16 ± 6 min. There were no significant differences between the 12 h EVP and 24 h EVP groups at perfusion end for the following parameters: MAP ($p=0.63$), pH ($p=0.77$), pO2 ($p=0.20$), venous pCO_2 ($p=0.22$), lactate ($p=0.28$), creatine kinase ($p=0.89$), or myoglobin ($p=0.95$). Electrolytes were also comparable at perfusion termination: sodium ($p=0.31$), potassium ($p=0.61$), and calcium ($p=0.29$).

After 12 h, flaps in the 24 h EVP group demonstrated a significant weight decrease (−4.5% [−4.6%, −4.1%] weight change), compared to the 12 h EVP group (1.2% [−1.1%, 1.6%] weight change) ($p=0.03$). At perfusion end, weight did not differ from baseline between the 24 h EVP (2.3% [0%, 3%]) and 12 h EVP groups ($p=0.37$). SCS flap weight was unchanged from baseline at 12 h ($p=0.954$) and 24 h ($p=0.616$). ICG revealed well-perfused flaps. H&E staining revealed preserved skin architecture without histopathological changes.

Conclusion: EVP preserved flaps for 24 h within physiologic parameters and without development of edema. EVP may extend preservation time for VCAs.

1 | Introduction

Abdominal wall transplantation provides a reconstructive solution for multivisceral transplant candidates with abdominal domain loss and extensive scarring [1–4]. This technique enables immediate closure, reducing morbidity from open abdomen management [3, 5, 6]. The cutaneous component allows for non-invasive rejection monitoring [7–10]. Since its advent, 38 patients have undergone this procedure [11–13].

The abdominal wall is usually procured before and transplanted after viscera, prolonging ischemia time [14]. Ischemia mitigation

strategies include revascularization via arteriovenous loops [15] or recipient non-dominant forearm vessels [14] during visceral transplantation.

Extracorporeal perfusion systems have been utilized to address ischemia-related damage over the past two decades [16–19]. While successful for solid organs [14, 18–21] and limbs, [8, 22–26] literature on EVP of VCAs is limited by brief durations (≤2 h) [8, 9, 13, 27] and hypothermic conditions (≤10°C) [10, 15, 28–30].

This study established a protocol for EVP of porcine abdominal wall allografts using acellular perfusate and compared it to static cold storage (SCS) controls. We hypothesized that EVP would preserve allografts in near-physiologic conditions for up to 24 h.

2 | Methods

2.1 | Animal Use

This study was approved by the Cleveland Clinic Institutional Animal Care and Use Committee (IACUC #00002418), which adhered to NIH guidelines for animal care.

Twenty superior epigastric artery (SEA) perforator-based abdominal flaps were procured from 10 Yorkshire pigs. Five flaps were preserved for 12 h and five flaps for 24 h using EVP with an oxygenated colloid solution containing HBOC-201 (HbO_2 Therapeutics, Souderton, PA) as oxygen carrier, while the contralateral flaps were kept at 4°C (SCS control) ($n = 10$).

2.2 | Flap Procurement

Animals were sedated and anesthetized with xylazine 2 mg/kg IM, ketamine 20 mg/kg IM, and 1%–4% isoflurane, maintained by continuous infusion of propofol IV (2–20 mg/kg/h), following endotracheal intubation. After standard preparation, a vertically oriented elliptical flap was marked using the cranial 2–3 nipples as landmarks for the course of the SEA, with a medial margin 1 cm lateral to the midline.

The SEA and vein were identified first dividing the fibers of rectus abdominis muscle cranial to the skin island. Next, the medial edge of the flap was incised and the plane deep to the panniculus carnosus muscle was followed. Dissection was carried out medial to lateral until the skin perforators of the SEA were identified. Three or more sizeable perforators were preserved and dissected through the rectus muscle until SEA was reached. The lateral flap margin was incised, and flap raised from distal to proximal. Next a paramedian incision was made on the sternal area, the lower four costal cartilages were exposed, then a 4 cm segment lateral to costosternal junction was removed. The intercostal muscles and residual perichondrium were divided to expose the cranial course of SEA, continuing cranially as internal thoracic artery. Once the flap was completely islanded on the vascular pedicle, infrared thermography (Fluke TiS Thermal Imager, Everett, WA) and indocyanine green (ICG) angiography (Stryker SPY Elite System, Munich, Germany) quantified flap perfusion and identified perfusion pattern (Figure 1). Finally, the pedicle was divided, and a 14-gauge cannula was inserted into the internal mammary artery. Flap weight was recorded before and after flushing with Krebs Ringer bicarbonate buffer (KRBB) solution until venous effluent was clear. Immediately, the flap was transferred to the EVP system. The contralateral flap was harvested and preserved as SCS control in a polyurethane bag at 4°C. The animal was then euthanized using Beuthanasia (0.22 mL/kg IV).

2.3 | Flap Perfusion

The EVP system included two circuits. The oxygenation circuit consisted of a peristaltic pump (Masterflex L/S, Avnator, USA), oxygenator and heat exchanger (Quadrox-I adult, Gettinge, USA), heat therapy pump (HT-1500, Adroit Medical, USA), reservoir (Terumo Cardiovascular Group, USA), and humidifier (7300R, Genstartech, USA) connected to mixture of 97.5 O_2 + 2.5 CO_2 gas supply. The perfusion circuit consisted of a peristaltic pump (Rabbit, Rainin Instruments, USA) sampling the oxygenated perfusate from the reservoir and supplying to the epigastric artery at a constant flow rate. The perfusion circuit contained inline temperature and pressure transducers (BioTrans, Biosensors International, USA).

The system was primed with 2 L of perfusate, consisting of 1.45 L of Hemoglobin-based oxygen carrier (HBOC)-201 (Hemopure, HbO2 Therapeutics, Souderton, PA) and 1.05 L of human albumin 25% solution. Vancomycin (250 mg), ceftazidime (500 mg), and cefazolin (250 mg) were added to the perfusate. Methylprednisolone (500 mg) was added for endothelial protection. Insulin and dextrose were added as needed to prevent an extracellular potassium shift and provide metabolic substrates to the tissue. Flow rates were gradually increased to maintain a mean arterial pressure (MAP) of 50 mmHg, starting from 10 mL/min at baseline, increasing to 15 mL/min by time point 3 h (TP3) and as needed afterwards. Vascular resistance was calculated through the hydrostatic variation of the Ohms equation R = (mean arterial pressure − venous pressure)/flow with the venous pressure set to 0 because the circuit had an open venous return. Perfusate exchanges (120 mL/min) were started at TP4 to maintain electrolyte concentrations within physiological ranges and minimize metabolite accumulation.

2.4 | EVP Monitoring

Tissue oxygen saturation was measured by near-infrared spectroscopy (ViOptix, Fremont, CA). Venous and arterial perfusate gases were sampled hourly (Abaxis i-STAT 1, Union City, CA). Arterial and venous oxygen content was calculated using the following formula: oxygen content = (1.36 × hemoglobin × O_2Sat/100) + (0.0031 × PO_2). Oxygen consumption was measured as O_2 consumption = flow × (arterial O_2 content—venous O_2 content). Oxygen uptake rate (OUR) was calculated as $(([O_2]_{in} - [O_2]_{out})/100) \times$ flow rate/flap weight, where $[O_2]_{in}$ is the oxygen content in mLO_2 /mL of arterial perfusate and $[O2]_{out}$ is the oxygen content in mLO_2/mL of venous perfusate. MAP (Phillips MP50, Phillips Medical Systems, USA) and flow rate (Transonic Systems Inc., USA) was continuously monitored, and flap weight was recorded every hour. Creatine kinase (CK), myoglobin and albumin levels were measured

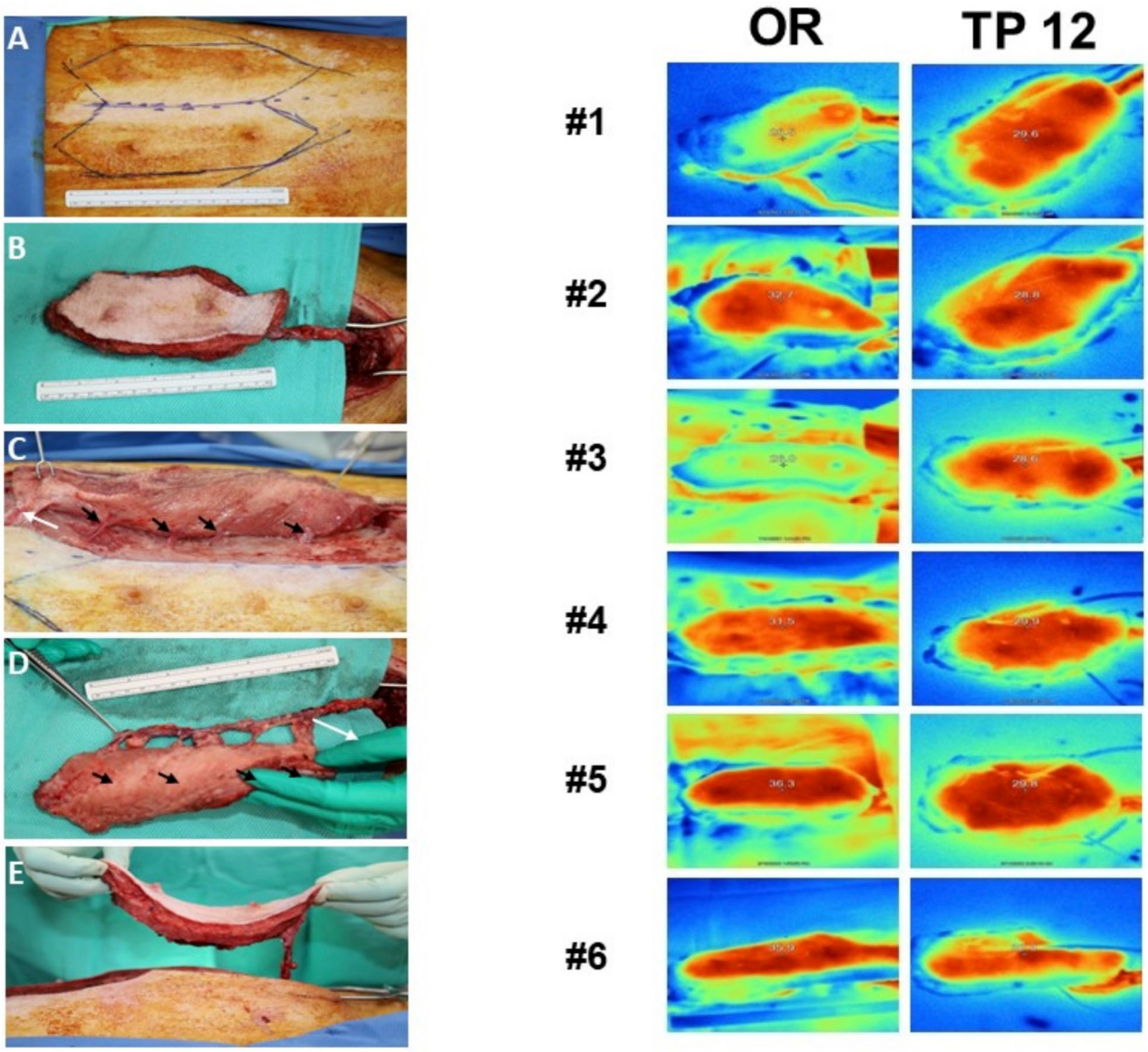

FIGURE 1 | Flap Procurement. (A) EVP and control flaps marked (22.0 ± 2.0 × 7.1 ± 0.6 cm), (B) Perforator vessels were preserved (black arrows), (C) Dissected flap with attached pedicle, (D) Elevated flap with perforators shown (black arrows), (E) Side view of flap elevation (dissected to rectus abdominis muscle). Probes for measuring flap tissue oxygenation and temperature are shown. [Color figure can be viewed at wileyonlinelibrary.com].

every 4 h (Siemens ADVIA 120 Hematology System, Munich, Germany). Surface temperature of the flap was assessed hourly by infrared thermography (Fluke TiS Thermal Imager, Everett, WA).

Skin biopsies from EVP and SCS flaps were collected at TP0 and every 6 h thereafter (Figure 2). Skin biopsies were taken and stored initially in 10% formalin for 48 h and then transferred to 70% ethanol and stained with hematoxylin and eosin. The slides were scanned by a high-resolution slide scanner (Aperio AT Turbo, Leica Biosystems, Buffalo Grove, IL) and evaluated by a pathologist blinded to the study groups. Histological evaluation of skin biopsies included perivascular inflammation, spongiosis, vacuolization of epidermal cells and epidermal necrosis. Immunohistochemistry staining for caspase-3 activity was performed using the Discovery ULTRA automated stainer from Roche Diagnostics (Indianapolis, IN). QuPath software (Version 0.3.0) [20] was used to quantify caspase-3 activity, [20] defined as a proportion of cleaved-caspase-3 positive cell nuclei to total cell nuclei. The algorithm for nuclei detection was based on a pixel size of 0.5 μm, DAPI staining intensity single threshold of 25, and an Opal 570 (Caspase-3 positive) staining intensity single threshold of 60. At perfusion endpoint, ICG angiography was used to investigate uniformity of the peripheral perfusion (Stryker SPY Elite System, Munich, Germany).

2.5 | Outcome Measures

Outcome measures, including perfusate dynamics (flow, pressure, and arterial resistance) temperature, gases (pO_2, pCO_2, SaO_2) metabolites (glucose, lactate, myoglobin, CK), electrolytes (Na^+, K^+, Ca^{++}), and flap weight, were monitored and

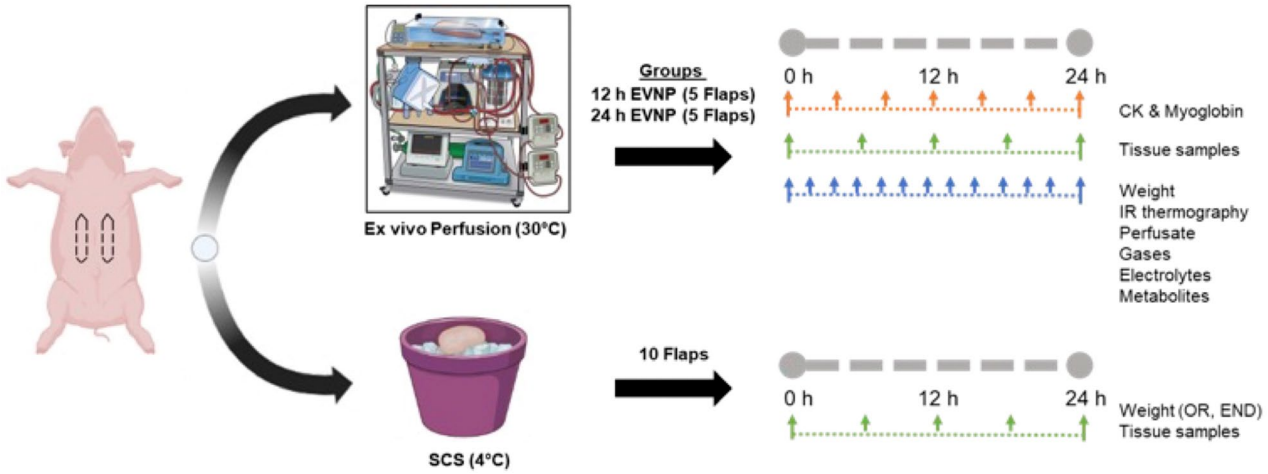

FIGURE 2 | Schematic of study design. Donor pig flaps were retrieved and either preserved at cold storage (4°C) or using ex vivo perfusion (30°C). [Color figure can be viewed at wileyonlinelibrary.com].

evaluated using Pearson correlations and paired *t*-tests. ICG angiography was utilized to analyze skin perfusion before division of the flap pedicle and after 12 h of EVP. Image analysis was performed using MATLAB software to obtain contours of pixel intensity regions. Percent of pixels with intensity above 200 were computed to determine the area of bright ICG regions to the total flap area.

2.6 | Statistical Analyses

We estimated a sample size of five flaps per study group to compare their respective outcomes based on previous studies with 95% confidence and 80% power to detect a 2% weight gain caused by edema, as 5% weight gain represents early decline of the machine perfused allograft [21]. Variables are reported as mean and standard deviation (mean ± SD) or median and interquartile range (median [IQR]). Data normality was assessed using the Jarque Bera test, and equality of variances using Levene's test. Kruskal-Wallis test with Dunn's post hoc pairwise comparison was performed for nonparametric data. For normally distributed continuous data, student *t*-tests or analysis of variance (ANOVA) with or without Welch modification, followed by Tukey post hoc pairwise comparison, were performed as appropriate. Pearson's correlation coefficients were generated to assess the correlation between continuous variables and presented as *r* and *p*-value. All statistical analyses were performed using IBM SPSS Statistics for MacOS, version 27 (IBM Corp., Armonk, NY, USA). A $p < 0.05$ was considered significant.

3 | Results

The average warm ischemia time was 16 ± 6 min, with no difference between EVP groups ($p = 0.82$). Initial flap weight was 191 ± 49 g and comparable between groups ($p = 0.17$). Average skin surface temperature throughout perfusion was 28.4°C ± 1.7°C in the 12 h EVP group and 30.7°C ± 1.4°C in the 24 h EVP group ($p < 0.0001$), although at perfusion end, there was no significant difference ($p = 0.70$).

3.1 | Perfusate Dynamics

Hemodynamic parameters are summarized in Figure 3. Perfusate flow was 10 ± 0 mL/min at baseline and increased to 15 ± 0 mL/min at TP12 in the 12 h EVP group ($p < 0.00001$). In the 24 h EVP group, flow increased from baseline 9 ± 4 mL/min to 18 ± 4 mL/min after 12 h perfusion ($p = 0.00009$). Flow remained steady at 18 ± 4 mL/min after 24 h ($p = 1.0$). Perfusate dynamics were stable throughout perfusion, with MAP maintained at 46 ± 16 mmHg ($r = -0.03$, $p = 0.72$) and vascular resistance slightly decreasing over time ($r = -0.39$, $p < 0.00001$).

3.2 | Gases

Perfusate gases are summarized in Table 1 and Figure 3. Mean arterial PaO_2 was not significantly different at perfusion end (471 ± 152 mmHg) in the 12 h EVP group ($p = 0.43$) compared to baseline (526 ± 84 mmHg). Mean arterial PaO_2 in the 24 h EVP group was also not significantly different between perfusion start (522 ± 25 mmHg) and end (575 ± 33 mmHg, $p = 0.21$). There were no differences in the mean PaO_2 between the two groups ($p = 0.23$) (Table 1).

$PaCO_2$ was 21 ± 2 mmHg at baseline, not changing significantly by perfusion end (20 ± 3 mmHg, $p = 0.45$) in the 12 h EVP group. $PaCO_2$ was also stable in the 24 h EVP flaps (TP0 21 ± 1 mmHg vs. TP24 20 ± 1 mmHg, $p = 0.18$) with no differences between the groups ($p = 0.45$). Both had 100% ± 0% tissue oxygen saturation at perfusion termination ($p = 1.00$).

OUR at baseline was 0.51 ± 0.16 mL/min*kg and did not significantly change by perfusion end in the 12 h EVP flaps (0.37 ± 0.23, $p = 0.62$). The average OUR in 24 h group was lower ($p < 0.0001$) but did not change significantly over 24 h (TP0 0.37 ± 0.48 mL/min*kg vs. TP24 0.16 ± 0.20, $p = 0.49$).

Venous PCO_2 in the 12 h EVP group was 23 ± 3 mmHg at baseline and trended downward to 19 ± 1 mmHg at TP12 ($p = 0.14$). In the 24 h EVP group, venous PCO_2 was 22 ± 3 mmHg at TP0 and displayed a downward trend to 18 ± 1 mmHg at TP24 ($p = 0.06$).

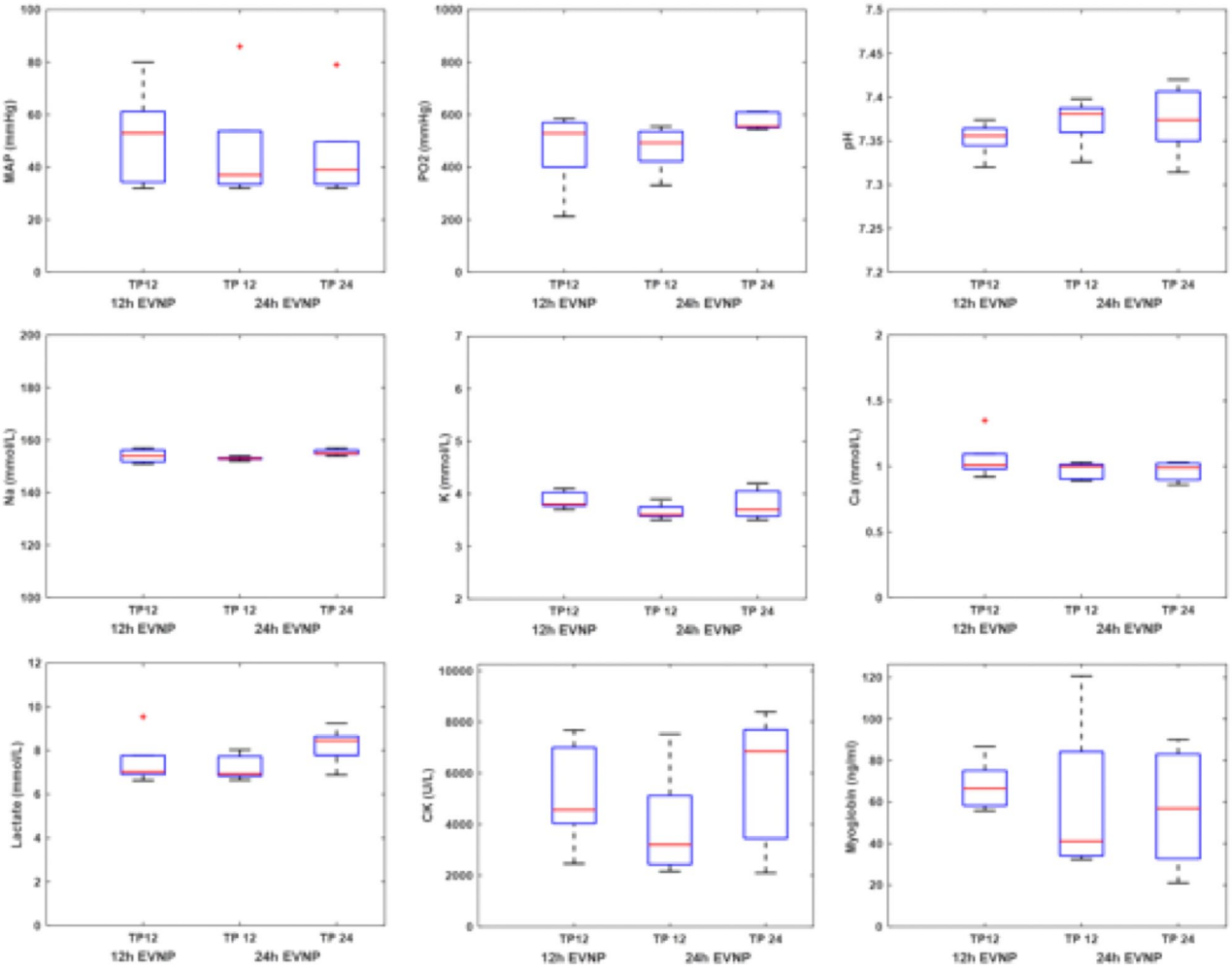

FIGURE 3 | Comparison of changes in perfusion pressure, and indicators of cellular integrity and metabolic activity (potassium, creatine kinase, lactate, tissue oxygenation, and pH) are shown in the perfused free flaps (see text for explanation). * signifies statistical significance [Color figure can be viewed at wileyonlinelibrary.com].

Perfusate pH was 7.36 ± 0.02 on average at TP0 and remained stable by the end of perfusion in the 12 h EVP group (7.37 ± 0.01, $p = 0.26$). In 24 h EVP, pH was also stable (TP0 7.38 ± 0.03 vs. TP24 7.38 ± 0.04, $p = 0.94$) (Table 1).

3.3 | Chemistry

Glucose was not different between treatment groups (12 h EVP 85 ± 11 mg/dL vs. 24 h EVP 87 ± 8 mg/dL, $p = 0.14$). Average venous lactate increased in both groups as perfusion progressed from a comparable baseline (12 h EVP 6.4 ± 0.2 vs. 6.2 ± 0.1 mmol/L, $p = 0.24$). At TP 12, the lactate levels were not significantly different in the two treatment groups (12 h EVP 7.5 ± 1.2 vs. 24 h EVP 7.2 ± 0.6, $p = 0.69$), but were increased from TP0 ($p = 0.04$, $p = 0.02$). For flaps perfused 24 h, the lactate levels were not significantly different at TP24 compared to TP12 (8.2 ± 0.9, $p = 0.18$).

CK was not significantly different at TP12 (4730 ± 2169 U/L) from baseline (Table 1) (1024 ± 766 U/L) for both treatment groups combined ($p = 0.24$). In the 24 h EVP group, the average CK was 5467 ± 2966 U/L at perfusion end and not significantly different from TP12 ($p = 0.85$).

Average venous methemoglobin trended upward from 20% ± 7% at TP0 to 43% ± 1% at TP12 in the 12 h EVP group ($p = 0.13$). For 24 h EVP flaps, the average venous methemoglobin also trended upward from 17% ± 5% at TP0 to 45.7 ± 9 at TP 24 ($p = 0.07$). Methemoglobin was higher in the 12 h compared to the 24 h EVP group ($p < 0.0001$). Myoglobin remained stable over time and comparable between groups ($p = 0.61$).

3.4 | Electrolytes

Average electrolyte concentrations for each group are shown in Table 1. Sodium concentration for both perfusion groups combined increased from baseline 150 ± 1.3 to 154 ± 3 mEq/L ($p = 0.006$) at TP12 and continued to increase from TP12 to TP24 (156 ± 1 mEq/L, $p = 0.04$). Average perfusate potassium concentration remained in a physiologic range (3.3 ± 1.0 to −3.8 ± 0.3 mEq/L), and comparable between groups ($p = 0.93$). Potassium increased in both groups from baseline to TP12 (12 h EVP $p = 0.002$, 24 h EVP $p = 0.02$). However, in the 24 h perfused flaps, potassium was not significantly different at endpoint compared to TP 12 ($p = 0.49$). Finally, calcium concentration increased over time in the 12 h EVP group

TABLE 1 | Comparison of parameters between the 12 h EVP group at 12 h and the 24 h EVP group at 12 and 24 h.

	12 h EVP	24 h EVP			
	TP12	TP12		TP24	
Parameter	Mean ± SD, median [IQR]	Mean ± SD, median [IQR]	*p*	Mean ± SD, median [IQR]	*p*
MAP (mmHg)	47 ± 13	44 ± 11	0.74	45 ± 19	0.63
Potassium (mmol/L)	3.9 ± 0.2	3.7 ± 0.2	0.06	3.8 ± 0.3	0.61
Sodium (mmol/L)	154 ± 2.5	153 ± 0.7	0.44	156 ± 1.1	0.31
Calcium (mmol/L)	1.1 ± 0.2	1.0 ± 0.1	0.31	1.0 ± 0.1	0.29
pH	7.37 ± 0.01	7.38 ± 0.03	0.60	7.38 ± 0.04	0.77
pO2 (mmHg)	471 ± 152	472 ± 88	0.98	575 ± 33	0.20
pCO2, venous (mmHg)	19 ± 1	19 ± 1	0.51	18 ± 1	0.22
Lactate, venous (mmol/L)	7.5 ± 1.2	7.2 ± 8.2	0.69	8.2 ± 0.9	0.28
CK (U/L)	5208 ± 2060	4133 ± 2456	0.51	5467 ± 2966	0.89
Myoglobin (ng/mL)	68 ± 12	65 ± 41	0.9	69 ± 29	0.95
Weight (g)	217 ± 48	167 ± 52	0.15	193 ± 60	0.52
Weight change (%)	1.2% [−1.1% to 1.6%]	−4.5% [−4.6% to −4.1%]	0.03	2.3% [0% to 3%]	0.37

Abbreviations: CK, creatine kinase; EVP, ex vivo perfusion; MAP, mean arterial pressure; pCO2, partial pressure of carbon dioxide; pO2, partial pressure of oxygen; TP, timepoint.

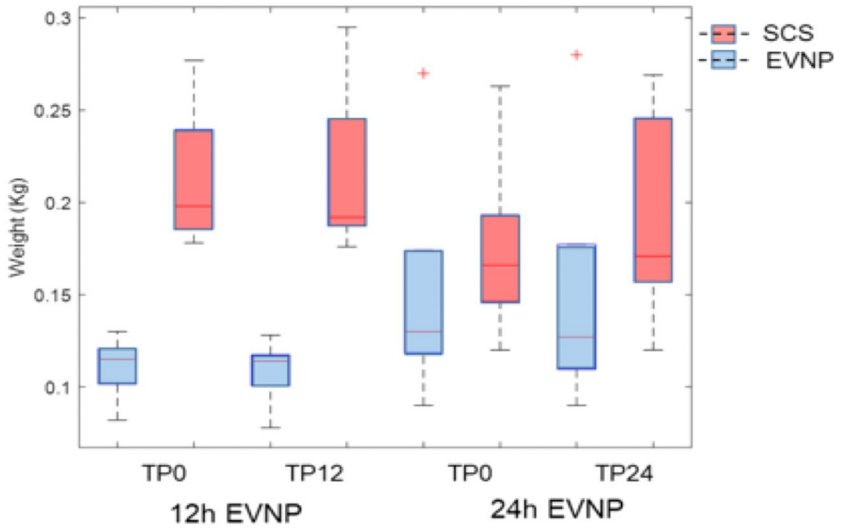

FIGURE 4 | Comparison of weight for flaps preserved in SCS and EVNP in 12 and 24 h groups. [Color figure can be viewed at wileyonlinelibrary.com].

($p = 0.009$) and was stable throughout perfusion in the 24 h EVP group ($p = 0.07$).

3.5 | Flap Parameters

Flap weight did not change significantly from beginning to end of perfusion in either group (12 h EVP TP0 214 ± 39 g vs. TP12 217 ± 48 g, $p = 0.50$; 24 h EVP TP0 175 ± 53 g vs. TP24 193 ± 60 g, $p = 0.31$; Table 1 and Figure 4). Furthermore, control flaps did not exhibit significant weight changes (TP0 136 ± 67 kg vs. TP12 135 ± 67 g, $p = 0.48$). The median percent weight change for SCS flaps was −1.1% [−2.5% to −0.4%]. From baselined to perfusion end, 12 h EVP flap weight changed by 1.2% [−1.1% to 1.6%] and 2.3% [0% to 3%] in 24 h EVP by perfusion end ($p = 0.37$). When compared to SCS controls, both 12 h EVP and 24 h EVP ($p = 0.04$) groups had higher percent weight gain, although this did not reach statistical significance for the 12 h EVP group ($p = 0.05$).

Infrared thermography confirmed peripheral perfusion (Figure 5). ICG angiography (Figure 6) revealed well-perfused flaps with regional differences. At endpoint, mean percent of pixels above 200 intensity was not significantly different between groups (12 h EVP 25% ± 8% vs. 24 h EVP 34% ± 5%,

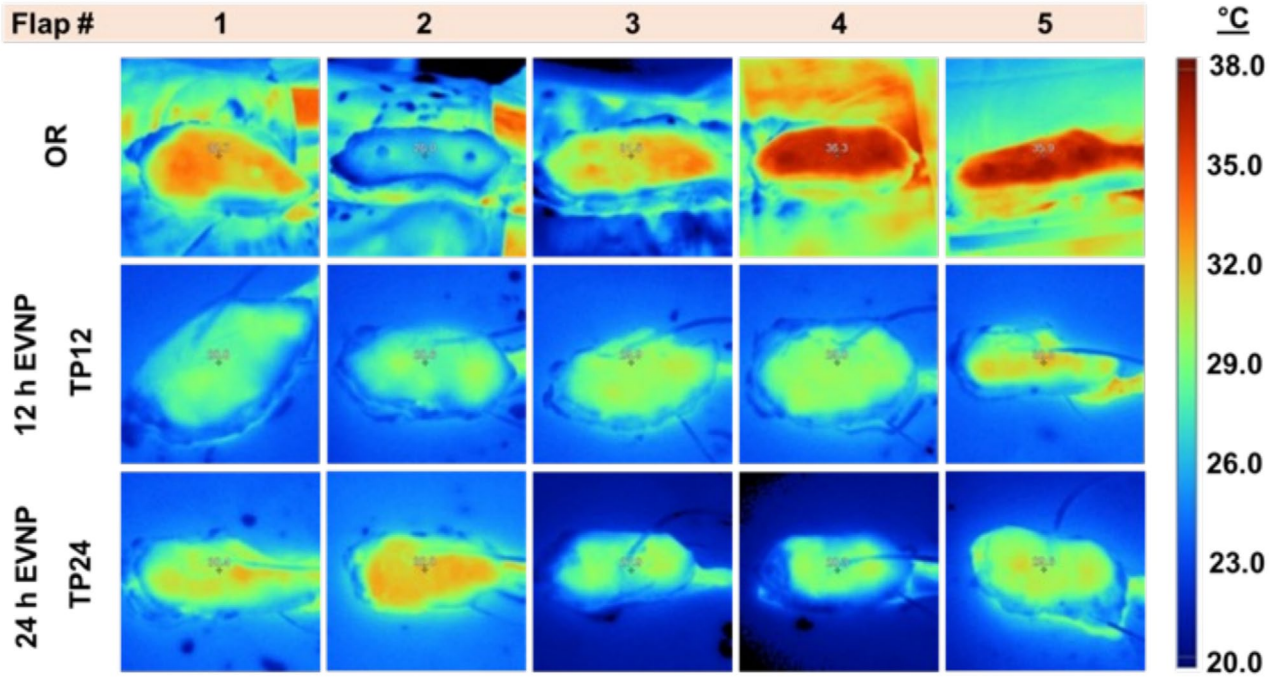

FIGURE 5 | Infrared thermography images of free flaps in the OR after the flap is islanded after 12 and 24 h of EVNP, shows well perfused flaps. [Color figure can be viewed at wileyonlinelibrary.com].

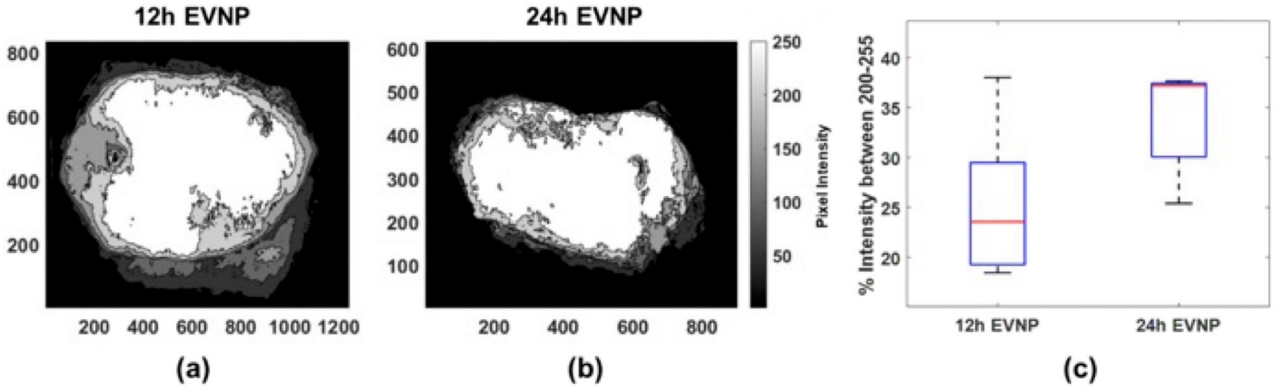

FIGURE 6 | Indocyanine green (ICG) fluorescence angiography of the perfused flaps at end point. Contour plots showing the ICG brightness regions. Scale bar presents the gray scale pixel intensity (a, b). Comparison of the percent pixel intensity between 200 and 255 pixels between 12 h EVNP and 24 h EVNP groups (c). [Color figure can be viewed at wileyonlinelibrary.com].

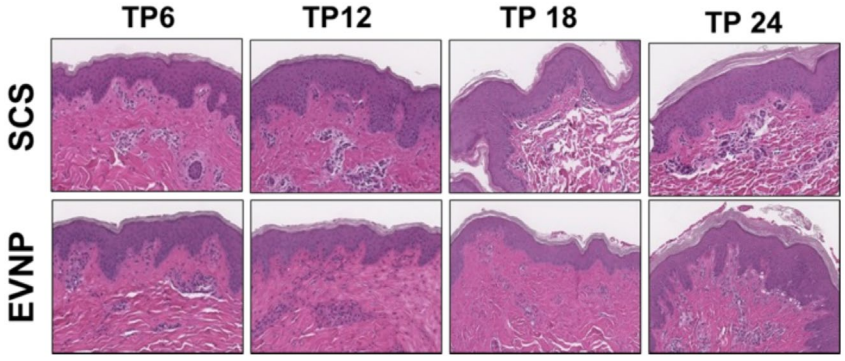

FIGURE 7 | H&E staining of skin biopsies of the 24 h EVNP group flaps preserved in SCS and EVSP. Biopsies in EVNP did not reveal damage, including perivascular inflammation, diffuse spongiosis, and vacuolization of epidermal cells or any signs of epidermal necrosis. Images shown at 20× magnification. [Color figure can be viewed at wileyonlinelibrary.com].

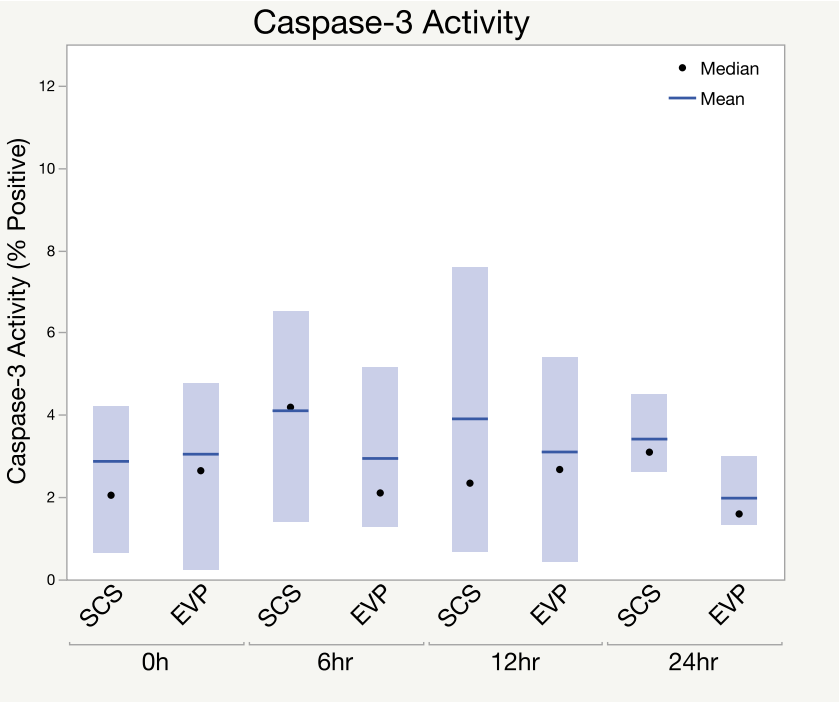

FIGURE 8 | Caspase-3 activity time profile of perfused skin biopsies and static cold storage (SCS) skin biopsies. There were no significant differences in Caspase-3 activity between SCS and perfusion. [Color figure can be viewed at wileyonlinelibrary.com].

$p = 0.08$). H&E histology of perfused skin biopsies revealed normal skin architecture, without any evident differences compared to baseline and SCS (Figure 7). The percentages of cells positive for caspase-3 activity in skin biopsies was not significantly different between SCS 0 h (2.05%, [0.65%–4.21%]), EVP 0 h (2.64% [0.24% to 4.77%]), SCS 12 h (2.81% [0.73% to 5.91%]), and EVP 12 h (2.67%, [0.56% to 3.86%]) ($p = 0.70$). Caspase-3 activity was higher after 24 h in the SCS group (3.09% [2.627%, 4.51%]) compared to EVP (1.59% [1.34% to 2.99%]), however this did not reach statistical significance (p = 0.08). There was no difference between baseline, SCS 24 h, and EVP 24 h ($p = 0.32$) (Figures 8 and 9). At perfusion end, there was no significant difference between EVP 12 h (2.67% [0.44% to 5.39%]) and EVP 24 h (1.59% [1.34% to 2.99%]) ($p = 0.61$).

4 | Discussion

Abdominal wall transplantation is a complex procedure involving allotransplantation of skin, fascial sheaths, and other tissues to replace damaged or missing abdominal structures [9, 15]. While this technique offers significant benefits over traditional reconstructive procedures, including immediate closure of the abdomen and monitoring of the intrabdominal multivisceral allograft rejection, it requires robust tissue preservation for success [14, 22]. While SCS is standard preservation method, it has time-dependent limitations [8, 9]. The unique logistics of this procedure make VCA preservation challenging, as abdominal wall tissue withstands ischemia throughout visceral organ procurement and transplantation [23]. In this study, EVP maintained vascular and metabolic integrity over 24 h, minimizing the damage seen with SCS. Flaps preserved with EVP exhibited stable weight and reduced edema formation compared to SCS controls, corroborating the ability of machine perfusion to sustain tissue viability over extended periods.

Ex vivo perfusion (EVP) systems have been developed to preserve other types of VCAs, but their use has not been extensively studied [17, 21, 24–26]. Traaholt et al. [31] in 1978 perfused a canine cutaneous flap based on superficial inferior epigastric perforators at 8°C for 80 min with 10% human serum albumin at 3.5–4.0 mL/min. The flap was then orthotopically replanted to the donor. Moderate edema noted directly after replantation subsided within 1 week.

Since the inception of EVP, several protocols for machine preservation of human and animal tissues have been described. Edema, manifesting as weight gain, precedes worsening arterial resistance and histological evidence of tissue damage [21, 27]. Flap weight gain up to 99.9% ± 22.5% of baseline has been documented after just 6 h of perfusion—although previous studies are heterogeneous, having used different perfusate temperatures, additives, flow rates, duration and flap anatomy [28, 32].

Vascularized composite flaps comprise tissues with varied energetic demands. For example, the endothelium, which supports vascular integrity, requires higher oxygenation and metabolic activity than adipose tissue. Our findings demonstrated that stable OUR likely reflect the preservation of energy-demanding endothelial components without compromising adipose viability. Additionally, glucose levels were maintained throughout perfusion, in part by manual addition of substrate and insulin (12 h EVP: 85 ± 11 mg/dL; 24 h EVP: 87 ± 8 mg/dL, $p = 0.14$), reflecting steady metabolic activity. This balance suggests that normothermic, oxygenated perfusion systems are particularly suited to meet the distinct metabolic needs of these heterogeneous tissues.

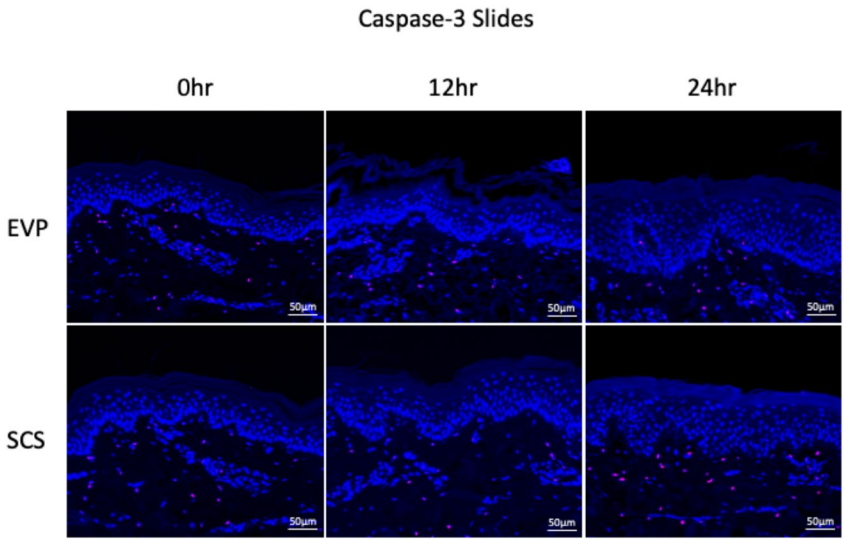

FIGURE 9 | Caspase-3-stained histological samples from both EVNP and SCS groups immediately after harvest, after 12 h, and after 24 h. [Color figure can be viewed at wileyonlinelibrary.com].

Dragu et al. harvested six porcine rectus abdominis flaps based on the inferior epigastric artery and preserved them using a 38.0°C ± 0.5°C perfusate composed of Jonosteril (Fresenius Jonosteri, Fresenius Kabi, Bad Homburg, Germany) and heparin for 2 h [29]. At a flow rate of 10 mL/min, the mean arterial pressure was maintained at 37 ± 5 mmHg; average weight increase after perfusion was 49.4% ± 5.9%.

Ozturk et al. perfused human deep inferior epigastric artery perforator flaps procured from discarded abdominoplasty tissue for 6 days (range 4–7 days). Flaps were perfused using fresh whole blood diluted with Lactated Ringer's and hydroxyethyl starch at a mean arterial flow 8–10 mL/min to maintain blood pressure of 90/100 mmHg and 34°C [30]. At endpoint, there was an average weight gain of 38% and the authors reported intact skin epithelium for the first 4 days, followed by complete epidermal loss by the seventh day. Active bleeding and capillary refill were noted throughout perfusion. Unlike these studies that reported significant edema formation and weight gains exceeding 30% after 6 h of perfusion, minimal weight changes (1.2% at 12 h, 2.3% at 24 h) in our study suggest intact endothelial integrity, as no significant interstitial fluid accumulation occurred during the perfusion span. This observation aligns with reduced edema and preserved vascular integrity.

Wolff et al. conducted the first clinical trials of extracorporeal free flap perfusion [33]. Ischemic and congested radial forearm flaps were perfused for 147 ± 52 (77–237) mins ($n = 8$) as a rescue strategy before anastomosis and compared to 30 radial forearm flaps where vascular anastomosis was performed immediately after flap harvest. Ex vivo perfused flaps had significantly reduced ischemia time and there was one failure in the control group. More recently, this group perfused ex vivo thinned anterolateral thigh ($n = 3$) and radial forearm ($n = 2$) flaps under the same protocol to investigate collateral formation in five patients with depleted recipient neck vessels [34]. There was one complete flap loss from perfusate infection, complete epithelial loss in two patients, venous congestion in one case, and healing without adverse events in the fifth. One patient healed by secondary intention, while the rest achieved stable wound coverage, and none required additional free flaps.

Slater et al. perfused porcine rectus abdominis myocutaneous flaps under both normothermic (34°C, heparinized autologous blood) and hypothermic (7°C, HTK, and University of Wisconsin (UW) acellular perfusate solutions) conditions for 24 h [35]. Flaps in all groups had reported weight gain "around 60%;" edema formed regardless of dexamethasone administration. Flaps that underwent machine perfusion with acellular perfusate at hypothermic temperatures showed fewer signs of cellular necrosis compared to the group perfused with autologous blood at 34°C, single IV flush controls, and SCS controls. However, the fundamental difference in perfusate composition is a confounder that cannot be discounted, as autologous blood contains white blood cells that drive inflammatory responses. Perfusate dynamics and oxygen consumption in our study (0.16 ± 0.20 mL/min/kg at 24 h) were consistent with findings by Slater et al. but demonstrated lower inflammatory responses with an acellular perfusate. Normothermic perfusion offers physiological advantages, including stable metabolic activity and reduced ischemic stress, as demonstrated by stable lactate levels from hours 12 to 24 of EVP in our study. Conversely, using hypothermic perfusion, Slater et al. have reported significant lactate elevation and diminished cellular activity due to limited oxygen delivery at lower temperatures. These findings suggest normothermia preserves metabolic integrity while mitigating edema formation compared to hypothermic approaches.

Several prior studies have also investigated subnormothermic and hypothermic perfusion protocols. Taeger et al. perfused five porcine rectus abdominus flaps based on deep inferior epigastric artery perforators for 6 h at room temperature using a hydroxyethyl starch solution and compared to five ischemic controls [36]. The perfused muscles remained metabolically active: measurements at the end of perfusion showed that flaps consumed glucose and pH decreased, and potassium increased. While Taeger et al. documented significant lactate

elevation during 6-h hypothermic perfusion, our findings demonstrated an increase in the first 12 h of perfusion before comparatively stable lactate levels from 12 to 24 h under normothermic conditions. This stability indicates efficient oxygenation and reduced anaerobic metabolism. Compared to ischemic controls, which lost the ability to generate a contractile force response between 3.5 and 5.25 h, perfused muscles were able to exert a force response and exhibited significantly lower proportions of apoptotic cells on annexin V (apoptotic nuclei) stained histology.

In a case study, Kolbenschlag et al. salvaged a myocutaneous latissimus dorsi free flap following acute arterial occlusion by 6 h of extracorporeal perfusion with a non-oxygenated isotonic heparinized saline solution (room temperature ischemia time throughout perfusion) at 3.6 mL/min [37]. Following perfusion, the flap was anastomosed and histology showed minimal cellular edema with occasional polymorphonuclear granulocytes 1 h after reperfusion. At 5-week follow-up, the flap had healed with 2 cm diameter tip necrosis. Our use of an oxygenated perfusate maintained tissue oxygenation, as evidenced by stable pO2 levels (575 ± 33 mmHg at 24 h) and reduced lactate accumulation. In contrast, Kolbenschlag et al.'s use of non-oxygenated perfusate resulted in oxygen depletion and anaerobic metabolism, compounding ischemic injury. These data underscore the critical role of oxygenation in preserving tissue viability during extended perfusion.

An abdominal wall replantation model by Kruit et al. was used to evaluate hypothermic perfusion for 18 h with UW solution ($n = 5$, 19.4°C ± 2.1°C) compared to a Histidine-Tryptophan-Ketoglutarate (HTK) solution ($n = 5$, 16.8°C ± 0.8°C) [28]. Flap weight did not increase during UW perfusion, as opposed to 56% weight gain during HTK perfusion. Within the 12 h period following replantation, weight increased in SCS and UW flaps (SCS mean + 47.3 g; 17%, UW: +66.8 g; 24%, $p = 0.674$), but decreased in the HTK group (mean − 72.6 g; −27%). The authors reported that two perfused flaps developed acute arterial occlusions and they ultimately reported a flap failure rate of 6.7% ($n = 1/15$).

Ex vivo machine perfusion has shown promise for preserving free flaps and VCAs in both animal models and human subjects. Clinical applications of EVP have shown improved outcomes compared to traditional cold storage methods. EVP using a normothermic acellular perfusate (HBOC-201) effectively preserved flaps for 24 h, maintaining physiologic perfusate chemistry and metabolite stability. Free skin flap temperatures were maintained within a viable range, as average human skin temperatures have been shown to vary between 29.8 ± 1.6 (sole of the left foot) and 34.7 ± 0.6 (anterior neck, face) [38]. Furthermore, preservation time by continuous perfusion in the present study exceeded that of prior studies in the ex vivo flap and VCA perfusion literature.

4.1 | Limitations

The main limitation of this study is that composite tissues were not transplanted after EVP. Comparison of the incidence and magnitude of reperfusion injury, as well as long-term VCA function, after transplantation can elucidate the threshold of observed injury that compromises viability once physiologic circulation is reestablished. The relationship between physiologic parameters during EVP, reperfusion phase, and long-term outcomes has yet to be established in this emerging field. Compared to ex vivo limb perfusion, EVP of other VCAs appears less challenging, as they lack defined fascial compartments [21]. Ex vivo flap perfusion, therefore, may require unique termination criteria based on tissue viability. However, extreme edema formation could acutely compromise microcirculation [28]. While weight stability during perfusion suggests intact endothelial permeability, vascular viability and functionality after reperfusion remain untested. Future studies will incorporate transplantation and replantation to correlate observed physiologic parameters during EVP with long-term tissue viability and functional outcomes.

5 | Conclusions

EVP effectively preserved porcine fasciocutaneous abdominal tissue for 24 h, maintaining physiologic parameters and tissue viability. EVP may serve as a superior alternative to cold storage for VCA preservation.

Author Contributions

A.M. contributed to concept/design, grant writing, data collection, statistics, data analysis/interpretation, and drafting of the article. V.L.K. contributed to concept/design, grant writing, data collection, and data analysis/interpretation. J.L. contributed to data collection, analysis, and interpretation. M.A. contributed to data collection, analysis, and interpretation. B.F. contributed to data collection, analysis, and interpretation. Y.K. contributed to data collection, analysis, and interpretation. L.M. contributed to data collection, analysis, and interpretation. R.K. contributed to data collection, analysis, and interpretation. J.R. contributed to data collection. D.J. contributed to data collection. R.F. contributed to data collection and critical revision of the article. P.S. contributed to concept/design, grant writing, and data collection. A.R. contributed to concept/design, grant writing, data collection, critical revision of the article, and approval of the article. B.B.G. contributed to concept/design, grant writing, data collection, data analysis/interpretation, drafting of the article, critical revision of the article, and approval of the article.

Acknowledgments

The authors have nothing to report.

Conflicts of Interest

The authors declare no conflicts of interest.

References

1. C. L. Cetrulo, Z. Y. Ng, J. M. Winograd, and K. R. Eberlin, "The Advent of Vascularized Composite Allotransplantation," *Clinics in Plastic Surgery* 44, no. 2 (2017): 425–429.

2. D. Light, N. Kundu, R. Djohan, et al., "Total Abdominal Wall Transplantation: An Anatomical Study and Classification System," *Plastic and Reconstructive Surgery* 139, no. 6 (2017): 1466–1473, https://journals.lww.com/plasreconsurg/Fulltext/2017/06000/Total_Abdominal_Wall_Transplantation__An.40.aspx.

3. N. G. Patel, I. Ratanshi, and E. W. Buchel, "The Best of Abdominal Wall Reconstruction," *Plastic and Reconstructive Surgery* 141, no. 1 (2018): 113e–136e.

4. V. P. Bustos, J. M. Escandón, E. Santamaría, et al., "Abdominal Wall Vascularized Composite Allotransplantation: A Scoping Review," *Journal of Reconstructive Microsurgery* 38, no. 6 (2022): 481–490.

5. K. L. Lak and M. I. Goldblatt, "Mesh Selection in Abdominal Wall Reconstruction," *Plastic and Reconstructive Surgery* 142, no. 3S (2018): 99S–106S.

6. J. M. Broyles, J. Berli, S. H. Tuffaha, et al., "Functional Abdominal Wall Reconstruction Using an Innervated Abdominal Wall Vascularized Composite Tissue Allograft: A Cadaveric Study and Review of the Literature," *Journal of Reconstructive Microsurgery* 31, no. 1 (2015): 39–44.

7. B. Kollar, P. Kamat, H. J. Klein, M. Waldner, R. Schweizer, and J. A. Plock, "The Significance of Vascular Alterations in Acute and Chronic Rejection for Vascularized Composite Allotransplantation," *Journal of Vascular Research* 56, no. 4 (2019): 163–180.

8. H. Giele, A. Vaidya, S. Reddy, G. Vrakas, and P. Friend, "Current State of Abdominal Wall Transplantation," *Current Opinion in Organ Transplantation* 21, no. 2 (2016): 159–164, https://journals.lww.com/co-transplantation/Fulltext/2016/04000/Current_state_of_abdominal_wall_transplantation.14.aspx.

9. S. H. Park and S. C. Eun, "Abdominal Wall Transplant Surgery," *Experimental and Clinical Transplantation* 16, no. 6 (2018): 745–750, https://pubmed.ncbi.nlm.nih.gov/30373506/.

10. G. E. Gondolesi and N. F. Aguirrea, "Techniques for Abdominal Wall Reconstruction in Intestinal Transplantation," *Current Opinion in Organ Transplantation* 22, no. 2 (2017): 135–141.

11. J. Lopez-Monclus, J. Muñoz-Rodríguez, C. San Miguel, et al., "Combining Anterior and Posterior Component Separation for Extreme Cases of Abdominal Wall Reconstruction," *Hernia* 24, no. 2 (2020): 369–379.

12. G. Trentadue, G. Kats-Ugurlu, T. Blokzijl, et al., "Safe and Successful Treatment of Acute Cellular Rejection of an Intestine and Abdominal Wall Transplant With Vedolizumab," *Transplantation direct* 6, no. 2 (2020): e527.

13. L. T. Reed, S. R. Echternacht, K. Shanmugarajah, R. Hernandez, H. N. Langstein, and J. I. Leckenby, "Twenty Years of Abdominal Wall Allotransplantation: A Systematic Review of the Short- and Long-Term Outcomes," *Plastic and Reconstructive Surgery* 150, no. 5 (2022): 1062E–1070E, https://pubmed.ncbi.nlm.nih.gov/36067486/.

14. H. Giele, C. Bendon, S. Reddy, et al., "Remote Revascularization of Abdominal Wall Transplants Using the Forearm," *American Journal of Transplantation* 14, no. 6 (2014): 1410–1416, https://pubmed.ncbi.nlm.nih.gov/24797611/.

15. D. Erdmann, A. Atia, B. T. Phillips, et al., "Small Bowel and Abdominal Wall Transplantation: A Novel Technique for Synchronous Revascularization," *American Journal of Transplantation* 19, no. 7 (2019): 2122–2126.

16. F. Messner, J. Grahammer, T. Hautz, G. Brandacher, and S. Schneeberger, "Ischemia/Reperfusion Injury in Vascularized Tissue Allotransplantation: Tissue Damage and Clinical Relevance," *Current Opinion in Organ Transplantation* 21, no. 5 (2016): 503–509, https://pubmed.ncbi.nlm.nih.gov/27495915/.

17. L. C. Burlage, S. N. Tessier, J. W. Etra, K. Uygun, and G. Brandacher, "Advances in Machine Perfusion, Organ Preservation, and Cryobiology: Potential Impact on Vascularized Composite Allotransplantation," *Current Opinion in Organ Transplantation* 23, no. 5 (2018): 561–567.

18. J. He, U. Z. Khan, L. Qing, P. Wu, and J. Tang, "Improving the Ischemia-Reperfusion Injury in Vascularized Composite Allotransplantation: Clinical Experience and Experimental Implications," *Frontiers in Immunology* 13 (2022): 998952.

19. T. Vogel, J. G. Brockmann, C. Coussios, and P. J. Friend, "The Role of Normothermic Extracorporeal Perfusion in Minimizing Ischemia Reperfusion Injury," *Transplantation Reviews (Orlando, Fla.)* 26, no. 2 (2012): 156–162, https://pubmed.ncbi.nlm.nih.gov/22459038/.

20. P. Bankhead, M. B. Loughrey, J. A. Fernández, et al., "QuPath: Open source software for digital pathology image analysis," *Scientific Reports* 7, no. 1 (2017): 16878, https://www.nature.com/articles/s41598-017-17204-5.

21. A. Meyers, S. Pandey, V. Kopparthy, et al., "Weight Gain Is an Early Indicator of Injury in Ex Vivo Normothermic Limb Perfusion (EVNLP)," *Artificial Organs* 47, no. 2 (2023): 290–301, https://pubmed.ncbi.nlm.nih.gov/36305734/.

22. A. C. Fortunato, R. S. Pinheiro, C. S. Matsumoto, et al., "Techniques for Closing the Abdominal Wall in Intestinal and Multivisceral Transplantation: A Systematic Review," *Annals of Transplantation* 27 (2022): e934595.

23. A. Atia, A. Hollins, R. F. Erdmann, et al., "Synchronous Abdominal Wall and Small-Bowel Transplantation: A 1-Year Follow-Up," *Plastic and Reconstructive Surgery. Global Open* 8, no. 7 (2020): e2995, https://journals.lww.com/prsgo/Fulltext/2020/07000/Synchronous_Abdominal_Wall_and_Small_bowel.29.aspx.

24. V. Fahradyan, d. Said SA, C. Ordenana, et al., "Extended Ex Vivo Normothermic Perfusion for Preservation of Vascularized Composite Allografts," *Artificial Organs* 44, no. 8 (2020): 846–855.

25. L. C. Burlage, A. G. Lellouch, C. B. Taveau, et al., "Optimization of Ex Vivo Machine Perfusion and Transplantation of Vascularized Composite Allografts," *Journal of Surgical Research* 270 (2022): 151–161, https://pubmed.ncbi.nlm.nih.gov/34670191/.

26. E. F. R. Duraes, M. Madajka, R. Frautschi, et al., "Developing a Protocol for Normothermic Ex-Situ Limb Perfusion," *Microsurgery* 38, no. 2 (2018): 185–194.

27. A. S. Kruit, H. Winters, J. van Luijk, M. C. J. M. Schreinemachers, and D. J. O. Ulrich, "Current Insights Into Extracorporeal Perfusion of Free Tissue Flaps and Extremities: A Systematic Review and Data Synthesis," *Journal of Surgical Research* 227 (2018): 7–16, https://pubmed.ncbi.nlm.nih.gov/29804865/.

28. A. S. Kruit, D. van Midden, M. C. Schreinemachers, et al., "Rectus Abdominis Flap Replantation After 18 h Hypothermic Extracorporeal Perfusion-A Porcine Model," *Journal of Clinical Medicine* 10, no. 17 (2021): 3858, https://pubmed.ncbi.nlm.nih.gov/34501304/.

29. A. Dragu, T. Birkholz, J. A. Kleinmann, et al., "Extracorporeal Perfusion of Free Muscle Flaps in a Porcine Model Using a Miniaturized Perfusion System," *Archives of Orthopaedic and Trauma Surgery* 131, no. 6 (2011): 849–855, https://link.springer.com/article/10.1007/s00402-010-1251-8.

30. M. B. Ozturk, T. Aksan, I. B. Ozcelik, et al., "Extracorporeal Free Flap Perfusion Using Extracorporeal Membrane Oxygenation Device: An Experimental Model," *Annals of Plastic Surgery* 83, no. 6 (2019): 702–708, https://journals.lww.com/annalsplasticsurgery/Fulltext/2019/12000/Extracorporeal_Free_Flap_Perfusion_Using.30.aspx.

31. L. Traaholt, R. Naas, and O. Slaattelid, "Perfusion and Reimplantation of a Free Skin Flap in a Dog. A Preliminary Report," *Scandinavian Journal of Plastic and Reconstructive Surgery* 12, no. 2 (1978): 163–164, https://pubmed.ncbi.nlm.nih.gov/694431/.

32. C. D. Taeger, O. Friedrich, R. E. Horch, et al., "Extracorporeal Perfusion—Reduced to a One-Way Infusion," *Clinical Hemorheology and Microcirculation* 79, no. 2 (2021): 257–267, https://pubmed.ncbi.nlm.nih.gov/28759964/.

33. K. D. Wolff, T. Mücke, A. Von Bomhard, et al., "Free Flap Transplantation Using an Extracorporeal Perfusion Device: First Three Cases," *Journal of Cranio-Maxillo-Facial Surgery* 44, no. 2 (2016): 148–154, https://pubmed.ncbi.nlm.nih.gov/26752222/.

34. K. D. Wolff, L. M. Ritschl, and A. von Bomhard, "In Vivo Perfusion of Free Skin Flaps Using Extracorporeal Membrane Oxygenation," *Journal of Cranio-Maxillo-Facial Surgery* 48, no. 1 (2020): 90–97, https://pubmed.ncbi.nlm.nih.gov/31874806/.

35. N. J. Slater, H. J. H. H. Zegers, B. Küsters, T. Beune, H. A. van Swieten, and D. J. O. O. Ulrich, "Ex-Vivo Oxygenated Perfusion of Free Flaps During Ischemia Time: A Feasibility Study in a Porcine Model and Preliminary Results," *Journal of Surgical Research* 205, no. 2 (2016): 292–295.

36. C. D. Taeger, O. Friedrich, R. E. Horch, et al., "Tissue Viability of Free Flaps After Extracorporeal Perfusion Using a Modified Hydroxyethyl Starch Solution," *Journal of Clinical Medicine* 9, no. 12 (2020): 1–11.

37. J. Kolbenschlag, M. Lescan, C. Bahrs, A. Bornemann, A. Daigeler, and R. Schäfer, "Transplantation of a Latissimus Dorsi Flap After Nearly 6 Hr of Extracorporal Perfusion: A Case Report," *Microsurgery* 41, no. 1 (2021): 75–78, https://pubmed.ncbi.nlm.nih.gov/32918759/.

38. C. M. Lee, S. P. Jin, E. J. Doh, D. H. Lee, and J. H. Chung, "Regional Variation of Human Skin Surface Temperature," *Annals of Dermatology* 31, no. 3 (2019): 349.